

Synthesis and Catalytic Oligomerization Activity of Chromium Catalysts of Ligand Systems with Switchable Connectivity

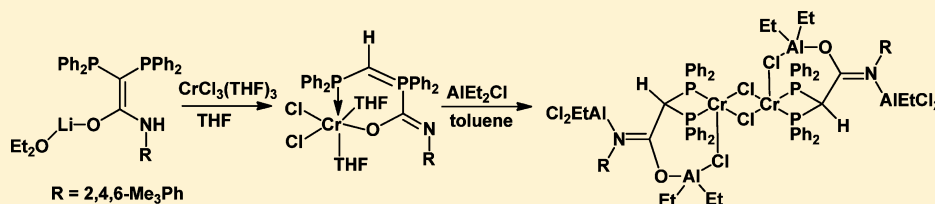
Shaneesh Vadake Kulangara,[†] Chris Mason,[‡] Michael Juba,[‡] Yun Yang,[†] Indira Thapa,[‡] Sandro Gambarotta,^{*,‡} Ilia Korobkov,[§] and Rob Duchateau^{*,†}

[†]Department of Chemical Engineering and Chemistry, Eindhoven University of Technology, P.O. Box 513, 5600 MB Eindhoven, The Netherlands

[‡]Department of Chemistry, University of Ottawa, Ottawa, Ontario K1N 6N5, Canada

[§]X-ray Core Facility, Faculty of Science, University of Ottawa, Ottawa, Ontario K1N 6N5, Canada

S Supporting Information



ABSTRACT: Nucleophilic attack of in situ generated bis(diphenylphosphino)methane (DPPM[−]) anion at CO₂, CyNCO, *t*-BuNCO, 2,6-(*i*-Pr)₂PhNCO, and 2,4,6-(Me₃)PhNCO resulted in the formation of the novel anionic ligands {[(Ph₂P)₂CHCO₂]₂Li(THF)₂]₂ (1), {[(Ph₂P)₂C=CNH(R)O]Li(OEt)₂]₂ (R = Cy (2), R = *t*-Bu (3)), [Ph₂PCH=P(Ph₂)C=N(2,6-*i*-Pr₂C₆H₃O)]Li(OEt)₂ (4), and {[(Ph₂P)₂C=CNH(2,4,6-Me₃C₆H₂O)]Li]_n (5), respectively. Ligand 4, however, showed a connectivity resulting from a nonclassical type of attack where the P atom acted as a nucleophilic center, thus affording a mixed-valent P(III)/P(V) species. Instead, the closely similar 5 showed a classical type of connectivity. The reaction of the in situ generated DPPM[−] anion with 1 and 0.5 equiv of CrCl₃(THF)₃ gave the chelated chromium complexes [HC(PPh₂)₂Cr(μ-Cl)₂Li(THF)₂]₂ (6) and [HC(PPh₂)₂Cr(μ-Cl)₂Li(THF)₂]₂·1.5THF (7), respectively. The reaction of ligand 1 with CrCl₂(THF)₂ afforded the dimeric [{ [(Ph₂P)₂C(H)CO₂]₂Cr(THF)₂ }]₂ (8), whereas the reaction of 3 with CrCl₃(THF)₃ resulted in the octahedral complex [(Ph₂P)₂C(H)C=N(*t*-Bu)O]CrCl₂(THF)₂·0.5THF·0.5(toluene) (9). The complexation of ligand 4 with CrCl₃(THF)₃ switched the connectivity to classical form and afforded the octahedral chromium complex [(Ph₂P)C(H)C=N(2,6-*i*-Pr₂C₆H₃O)]CrCl₂(THF)₂·1.5THF (10). In contrast, the reaction of the classical ligand 5 with CrCl₃(THF)₃ resulted in [(Ph₂P)C(H)=P(Ph₂)C=N(2,4,6-Me₃C₆H₂O)]Cr(THF)₂Cl₂ (11) with a nonclassical type of connectivity. Reaction of 11 with DEAC switched the connectivity back to a classical type, affording { (EtCl₂Al)[(Ph₂P)₂C(H)C=N(2,4,6-Me₃C₆H₂O)AlEt₂](μ-Cl)Cr₂(μ-Cl)₂}(toluene) (12). The catalytic behavior of all of these complexes has been assessed under different oligomerization conditions, and it was found that the modification of the DPPM framework with cumulenes considerably enhances their catalytic performance in comparison to catalysts 6 and 7. In any event, a Schultz–Flory distribution of oligomers was obtained. However, the in situ catalytic testing of ligands 2–4 using Cr(acac)₃ as metal precursor and DMAO as cocatalyst, in methylcyclohexane, switched the catalytic behavior to selective formation of 1-hexene and 1-octene (no higher liquid oligomers) along with a significant amount of narrowly dispersed, low-molecular-weight polyethylene wax. Interestingly, the precatalyst 12 showed self-activating trimerization capability with moderate activity.

INTRODUCTION

Catalytic ethylene oligomerization is an industrially relevant process.¹ The fact that the fractionation of the oligomerization mixture to extract the most requested α -olefins (1-hexene and 1-octene) is an energy-intensive process motivates the search for selective catalytic systems. As a result of intense research activity in this field, several selective ethylene trimerization catalysts,^{2–6} as well as a few ethylene tetramerization systems, have been discovered.⁷

Among the elements displaying catalytic behavior for ethylene oligomerization/polymerization, chromium occupies a unique position, since it provides commercially viable poly-

tri-, and tetramerization catalytic systems.⁶ The commonly accepted mechanism for selective ethylene oligomerization is a redox metallacycle mechanism,⁸ where a two-electron oxidative addition of ethylene to chromium forms an expandable chroma metallacycle. The active oxidation state of chromium responsible for the selectivity has been the center of a debate due to the ambiguities generated by the redox dynamism of this metal.^{8f,9–13} Different redox couples^{10–12} have been proposed, but recent work has clearly pointed out that Cr(I) is most likely

Received: July 19, 2012

Published: August 27, 2012

the species responsible for catalyst selective behavior.¹³ Therefore, if a selective tri- or tetramerization system is being sought, the main challenge is to stabilize the highly reactive monovalent oxidation state. In turn, this relates to a judicious choice of the ancillary ligand framework and donor atom combination. However, designing catalysts which may distinguish between selective tri- and tetramerization remains a great challenge.

The BP Chemicals and Sasol PNP chromium complexes, stabilized by neutral RN(PAR₂)₂ ligands, have marked a milestone in this field. These catalysts oligomerize ethylene with high selectivity toward either 1-hexene or 1-octene, depending on the ligand substituents (Ar = 2-OMe-C₆H₄, C₆H₅, respectively).^{4,7a} Further replacements of the heteroatom combinations or modifications of the ligand frameworks¹⁴ also produced highly selective ethylene trimerization catalysts. We also have reported a series of Cr(III) and Cr(II) complexes of NPN¹⁵ and NP¹⁶ ligands, which showed switchable catalytic behavior. Last but not least, SK-Energy reported a selective ethylene tetramerization system based on substituted bis(diphenylphosphino)ethane ligands, producing 1-octene with 77% selectivity.^{7b} Recently, we found that the chromium(III) complexes of the [PPh₂NR(CH₂)₃NRPPH₂] ligand are also capable of producing 1-octene with record selectivity.^{7c}

From this collection of results, it is clear that the presence of phosphorus donor atoms in the ligand scaffold of these heteroditopic ligands is an important prerequisite. However, the simpler bis(diphenylphosphino)methane (DPPM) ligand, in combination with CrCl₃(THF)₃ and activated with MMAO, only produces a Schultz–Flory distribution of oligomers with very low activity.¹⁷ This is in spite of its similarity to the PNP system in terms of bite angle, steric encumbrance, and donor atoms and also to the relationship with the SK-Energy diphosphine system. Conversely, Wass and co-workers¹⁸ reported that activation of bis(diphenylphosphino)methane-stabilized tetracarbonylchromium via one-electron oxidation provides a selective ethylene oligomerization catalyst producing mainly 1-hexene and 1-octene with a higher selectivity toward 1-octene in comparison to 1-hexene.

We are currently engaged in a systematic screening of families of diversified ligand systems containing various combinations of donor functions and ligand scaffolds containing the ability for retaining alkyl aluminate residues. This last point is of interest in the ultimate view of obtaining self-activating catalytic systems.^{9,13,15} For this work, we have examined deprotonated bis(diphenylphosphino)methane as the starting point and reacted it with CO₂ and isocyanate to probe geometrical arrangements not previously examined. It was argued that the phosphorus donor atoms might be central to the stabilization of the highly desirable lower oxidation states of chromium. At the same time, hard donors such as oxygen and nitrogen could aid in the retention of aluminum residues.^{13,14c,15,16} The anionic character of these ligands, in combination with the ability of the system to form zwitterionic species, was also regarded as beneficial for imparting robustness to the complexes and providing sufficient electrophilicity to the metal center. Herein we describe our observations.

EXPERIMENTAL SECTION

General Procedures. All air- and/or water-sensitive reactions were performed under a nitrogen atmosphere, in oven-dried flasks using standard Schlenk type techniques. Anhydrous solvents were obtained by means of a multiple column purification system.

CrCl₂(THF)₂ and CrCl₃(THF)₃ were prepared according to published procedures.¹⁹ Bis(diphenylphosphino) methane, CyNCO, *t*-BuNCO, 2,4,6-(Me₃)PhNCO, 2,6-(*i*-Pr)₂PhNCO, and lithium and aluminum reagents were purchased from Sigma Aldrich and used as received. Unless stated otherwise, the ¹H, ¹³C{¹H}, and ³¹P{¹H} NMR spectra were recorded on a Bruker 300 spectrometer at 300.13, 75.47, and 121.49 MHz, respectively, at 298 K. DMSO-*d*₆, dried with 4 Å molecular sieves and stored under nitrogen, was used for all the NMR measurements. All chemical shifts are given in ppm and referenced to SiMe₄. Elemental analyses were carried out with a Perkin-Elmer 2400 CHN analyzer. Molecular weights and molecular weight distributions of the polyethylenes were determined by means of high-temperature SEC on a PL-GPC210, equipped with refractive index and viscosity detectors and a 3 × PLgel 10 μm MIXED-B column set, at 160 °C with 1,2,4-trichlorobenzene as solvent. BHT and Irganox have been used as antioxidants. The molecular weights of the polyethylenes produced were referenced to linear polyethylene standards. Oligomerization data were analyzed by ¹H NMR spectroscopy for activity and GC-MS for reaction mixture composition. Gas chromatography of oligomerization products was conducted on a Varian 450-GC equipped with an autosampler.

General Oligomerization Procedure. All oligomerizations were performed in a 250 mL Büchi reactor. The reactor was dried in an oven at 120 °C for 2 h prior to each run and then evacuated for 1/2 h and rinsed with argon three times. After that, the reactor was loaded with toluene and the desired amount of cocatalyst. After the solution was stirred for 10 min, it was saturated with ethylene. The reactor was temporarily depressurized to allow injection of the catalyst solution into the reactor under an argon flow, after which the reactor was immediately repressurized to the desired set point. The temperature of the reactor was kept as constant as possible by a thermostat bath. After 30 min reaction time and cooling to 0 °C, the reaction mixture was depressurized and a mixture of ethanol and dilute hydrochloric acid was subsequently injected to quench the reaction. The polymer was separated by filtration and dried at 60 °C for 18 h under reduced pressure prior to molecular weight determination.

Computational Method. Geometry optimizations were performed using the Gaussian 09 program package without symmetry constraints, using the unrestricted B3LYP hybrid functional and double-ζ basis set 6-31G(d,p). Frequency analyses were carried out on the resulting geometries to verify the nature of stationary points (no imaginary frequencies).

X-ray Crystallography. Suitable crystals were selected, mounted on a thin, glass fiber with paraffin oil, and cooled to the data collection temperature. Data were collected on a Bruker AXS SMART 1 k CCD diffractometer. Data collection was performed with three batch runs at ψ = 0.00° (600 frames), at ψ = 120.00° (600 frames), and at ψ = 240.00° (600 frames). Initial unit-cell parameters were determined from 60 data frames collected at different sections of the Ewald sphere. Semiempirical absorption corrections based on equivalent reflections were applied. The systematic absences and unit-cell parameters were consistent for the reported space groups. The structures were solved by direct methods, completed with difference Fourier syntheses, and refined with full-matrix least-squares procedures based on *F*². All non-hydrogen atoms were refined with anisotropic displacement parameters. All hydrogen atoms were treated as idealized contributions. All scattering factors and anomalous dispersion factors are contained in the SHELXTL 6.12 program library.

Synthesis of {[(Ph₂P)₂C(H)CO₂Li(THF)₂]}₂ (1). A solution of bis(diphenylphosphino)methane (13.4 mmol, 5.1 g) in THF (130 mL) was treated with *n*-BuLi (13.4 mmol, 2.5 M, 5.3 mL). The resulting yellow solution was stirred for 3 h. The solution was then saturated with CO₂ for a period of 3 h and then kept at −35 °C for 2 days, thus affording colorless crystals of 1. Yield: 3.2 g, 5.5 mmol, 41%. ¹H NMR: δ 7.08–7.55 (m, 20H; Ar H), 4.00 (br, 1H; P₂CH). ¹³C{¹H} NMR: δ 48.05 (PCP), 128.3, 133.8, 139.7 (Ar C, Ph), 170.2 (*t*-C, CO₂). ³¹P{¹H} NMR: δ −16.13.

Synthesis of {[(Ph₂P)₂C=CNH(Cy)O]Li(OEt)₂]}₂ (2). A solution of bis(diphenylphosphino)methane (10 mmol, 3.8 g) in diethyl ether (100 mL) was treated with *n*-BuLi (10.1 mmol, 2.5 M, 4.1 mL) at

room temperature. After the addition was completed, the solution was stirred for 3 h. Cyclohexyl isocyanate (10 mmol, 1.3 mL) was added to the yellow solution, and the mixture was stirred for 3 h and subsequently kept at $-35\text{ }^{\circ}\text{C}$ for 2 days, affording colorless crystals of **2**. Yield: 5.4 g, 4.6 mmol, 46%. ^1H NMR: δ 0.5–1.3 (m, 10H; Cy H), 3.3 (m, 1H; *ipso* H Cy), 4.8 (br, 1H; NH), 7.1–7.3 (m, 20H; Ar H). $^{13}\text{C}\{^1\text{H}\}$ NMR: δ 25.9 (Cy CH_2), 47.5 (*ipso* C Cy), 132, 126, 125 (Ar C), 144.8 (PCP), 172.8 (*t*-C-NCO). $^{31}\text{P}\{^1\text{H}\}$ NMR: δ -12.04 .

Synthesis of $\{[(\text{Ph}_2\text{P})_2\text{C}=\text{CNH}(\text{t-Bu})\text{O}]\text{Li}(\text{OEt})_2\}_2$ (3**).** A solution of bis(diphenylphosphino)methane (12.8 mmol, 4.9 g) in THF (100 mL) was treated with *n*-BuLi (13.5 mmol, 2.5 M, 5.6 mL). The resulting yellow solution was stirred for 3 h. *tert*-Butyl isocyanate (12.8 mmol, 1.3 g) was then added, resulting in the immediate precipitation of a white powder. The precipitate was washed three times with cold hexanes and analyzed after drying under vacuum for 12 h. Yield: 4.8 g, 9.8 mmol, 76%. ^1H NMR: δ 0.79 (s, 9H; $(\text{CH}_3)_3\text{C}$), 3.79 (br, 1H; NH), 7.1–7.6 (m, 20H; Ar H). $^{13}\text{C}\{^1\text{H}\}$ NMR: δ 29.16 (CH_3), 49.4 (CCH_3), 126.85, 127.34, 132.58 (Ar C, Ph), 145.23 (PCP), 174.0 (NCO). $^{31}\text{P}\{^1\text{H}\}$ NMR: δ -13.9 .

Synthesis of $[\text{Ph}_2\text{PCH}=\text{P}(\text{Ph}_2)\text{C}=\text{N}(2,6\text{-}i\text{-Pr}_2\text{C}_6\text{H}_3\text{O})\text{Li}(\text{OEt})_2$ (4**).** A solution of bis(diphenylphosphino)methane (10 mmol, 3.8 g) in diethyl ether (100 mL) was treated with *n*-BuLi (10 mmol, 2.5 M, 4.1 mL). After the addition, the suspension was stirred for 1 h, resulting in a clear yellow solution. Neat 2,6-diisopropylphenyl isocyanate (10 mmol, 2.1 g) was added, and the mixture was stirred for another 5 h. The resulting yellow solution was then kept at $-35\text{ }^{\circ}\text{C}$ for 2 days, affording colorless crystals of **4**. Yield: 3.4 g, 4.6 mmol, 46%. ^1H NMR: δ 0.61 (d, 12H; CH_3), 2.63 (m, 2H; *ipso*-CH), 4.26 (t, 1H; PCHP), 6.5–7.7 (m, 23H; Ar H). $^{13}\text{C}\{^1\text{H}\}$ NMR: δ = 24.2 (*i*-Pr CH_3), 26.89 (*i*-Pr CHCH_3), 46.01 (PCP), 164.9 (*t*-C, ArNCO), 151.2, 140.6, 134.4, 127.8 (ArCNCO), 127.8, 127.4, 133.8 (PPh). $^{31}\text{P}\{^1\text{H}\}$ NMR: δ -8 , -24 .

$\{[(\text{Ph}_2\text{P})_2\text{C}=\text{CNH}(2,4,6\text{-Me}_3\text{C}_6\text{H}_2)\text{O}]\text{Li}\}_n$ (5**).** A solution of bis(diphenylphosphino)methane (13.4 mmol, 5.13 g) in diethyl ether (130 mL) was treated with *n*-BuLi (13.4 mmol, 2.5 M, 5.3 mL). After the addition, the solution was stirred for 1 h, affording a clear yellow solution. 2,4,6-Trimethylphenyl isocyanate (13.4 mmol, 2.15 g) was added to the stirred solution. After 1 h, **5** separated out as a white precipitate, which was isolated by filtration and recrystallized from THF (3.69 g, 5.7 mmol, 43%). ^1H NMR (500 MHz, $20\text{ }^{\circ}\text{C}$): δ 6.9–7.9 (20H, P-(C_6H_6)), 6.4 (2H, $\text{C}_6\text{H}_2(\text{CH}_3)_3$), 4.5 (1H, NH), 1.6 (9H, $\text{C}_6\text{H}_2(\text{CH}_3)_3$). $^{31}\text{P}\{^1\text{H}\}$ NMR: δ -12.5 .

Synthesis of $[\text{HC}(\text{PPh}_2)_2\text{Cr}(\mu\text{-Cl})_2\text{Li}(\text{THF})_2]_2$ (6**).** A solution of bis(diphenylphosphino)methane (1.0 mmol, 382 mg) in THF (6 mL) was treated with *n*-BuLi (1.1 mmol, 2.5 M, 0.4 mL), and the resulting yellow solution was stirred for 3 h at room temperature. A suspension of $\text{CrCl}_3(\text{THF})_3$ (1 mmol, 375 mg) in THF was then added, resulting in a green mixture which was stirred for 2 h. After centrifugation, the resulting green solution was then kept at room temperature for 4 days, forming pale green crystals of **6**. Yield: 580 mg, 0.66 mmol, 66%. Anal. Calcd (found) for $\text{C}_{41}\text{H}_{33}\text{Cl}_4\text{CrLi}_2\text{O}_4\text{P}_2$: C, 55.9 (56.01); H, 6.02 (6.10). $\mu_{\text{eff}} = 3.92\ \mu_{\text{B}}$.

Synthesis of $[\text{HC}(\text{PPh}_2)_2\text{Cr}(\mu\text{-Cl})_2\text{Li}(\text{THF})_2]\cdot 1.5\text{THF}$ (7**).** A solution of bis(diphenylphosphino)methane (1.0 mmol, 382 mg) in THF (6 mL) was treated with *n*-BuLi (1.1 mmol, 2.5 M, 0.4 mL), and the resulting yellow solution was stirred for 3 h at room temperature. A THF suspension of $\text{CrCl}_3(\text{THF})_3$ (0.5 mmol, 190 mg) was then added to this solution, affording a brown mixture which was stirred for 8 h. The solvent was removed under vacuum, and the residue was redissolved in toluene. After centrifugation, the supernatant liquid was evaporated. The dark brown residue was redissolved in THF and kept at $-35\text{ }^{\circ}\text{C}$ for 7 days, affording brown crystals of **7**. Yield: 280 mg, 0.24 mmol, 24%. Anal. Calcd (found) for $\text{C}_{64}\text{H}_{70}\text{Cl}_2\text{CrLiO}_{3.50}\text{P}_4$: C, 66.82 (66.90); H, 6.09 (6.10). $\mu_{\text{eff}} = 3.82\ \mu_{\text{B}}$.

Synthesis of $\{[(\text{Ph}_2\text{P})_2\text{C}(\text{H})\text{C}(\text{O})_2]\text{Cr}(\text{THF})_2\}_2$ (8**).** A colorless solution of the ligand **1** (1.157 g, 1.0 mmol) in THF was mixed with a suspension of $\text{CrCl}_2(\text{THF})_2$ (266 mg, 1 mmol) in THF, and the resulting pale blue solution was stirred for 4 h. The solvent was then removed under vacuum, the residue was redissolved in fresh THF (4 mL), and the resulting mixture was centrifuged. After centrifugation,

the supernatant liquid was separated and concentrated and kept at $-35\text{ }^{\circ}\text{C}$, thus affording pale blue crystals of **8**. Yield: 837 mg, 0.35 mmol, 35%. Anal. Calcd (found) for $\text{C}_{136}\text{H}_{148}\text{Cr}_2\text{O}_{16}\text{P}_8$: C, 68.28 (68.21); H, 6.19 (6.21). $\mu_{\text{eff}} = 3.91\ \mu_{\text{B}}$.

Synthesis of $\{[(\text{Ph}_2\text{P})_2\text{C}(\text{H})\text{C}=\text{N}(\text{t-Bu})\text{O}]\text{-CrCl}_2(\text{THF})_2\cdot 0.5\text{THF}\cdot 0.5(\text{toluene})\}_2$ (9**).** A white suspension of **3** (489 mg, 1.0 mmol) in THF was mixed with a suspension of $\text{CrCl}_3(\text{THF})_3$ (375 mg, 1 mmol) in THF, and the resulting pale green solution was stirred for 1 h. The solvent was then removed under vacuum, and the residue was suspended in toluene. After centrifugation, the supernatant liquid was separated, concentrated, and kept at room temperature for 7 days, thus affording pale green crystals of **9**. Yield: 400 mg, 0.48 mmol, 48%. Anal. Calcd (found) for $\text{C}_{43.50}\text{H}_{53}\text{Cl}_2\text{CrNO}_{3.50}\text{P}_2$: C, 62.83 (62.86); H, 6.38 (6.29); N, 1.68 (1.70). $\mu_{\text{eff}} = 3.89\ \mu_{\text{B}}$.

Synthesis of $\{[(\text{Ph}_2\text{P})\text{C}(\text{H})\text{C}=\text{N}(2,6\text{-}i\text{-Pr}_2\text{C}_6\text{H}_3\text{O})]\text{-CrCl}_2(\text{THF})_2\cdot 1.5\text{THF}\}_2$ (10**).** A colorless solution of **4** (741 mg, 1 mmol) in THF was treated with $\text{CrCl}_3(\text{THF})_3$ (375 mg, 1 mmol), and the resulting green mixture was stirred for 4 h. The solvent was removed under vacuum, and the residue was suspended in toluene. After centrifugation, the supernatant liquid was evaporated and the green solid redissolved in THF. Green crystals of **10** were obtained by keeping the solution at $-30\text{ }^{\circ}\text{C}$ for 1 week. Yield: 560 mg, 0.58 mmol, 58%. Anal. Calcd (found) for $\text{C}_{52}\text{H}_{66}\text{Cl}_2\text{CrNO}_{4.50}\text{P}_2$: C, 64.89 (64.72); H, 6.90 (6.88); N, 1.45 (1.49). $\mu_{\text{eff}} = 3.82\ \mu_{\text{B}}$.

Synthesis of $\{[(\text{Ph}_2\text{P})\text{C}(\text{H})=\text{P}(\text{Ph}_2)\text{C}=\text{N}(2,4,6\text{-Me}_3\text{C}_6\text{H}_2)\text{O}]\text{-Cr}(\text{THF})_2\text{Cl}_2\}_2$ (11**).** A suspension of **5** (2 mmol, 1.29 g) in THF (60 mL) was mixed with $\text{CrCl}_3(\text{THF})_3$ (2 mmol, 748 mg). Upon completion of the addition, the solution was stirred for 15 min, affording a dark brown solution. The solution was centrifuged, and the supernatant liquid was concentrated in vacuo and allowed to crystallize at $-37\text{ }^{\circ}\text{C}$, which afforded brown crystals of **11**. Yield: 0.99 g, 1.2 mmol, 61%. Anal. Calcd (found) for $\text{C}_{51}\text{H}_{64}\text{Cl}_2\text{CrNO}_5\text{P}_2$: C, 64.04 (64.08); H, 6.69 (6.72); N, 1.46 (1.48). $\mu_{\text{eff}} = 3.82\ \mu_{\text{B}}$.

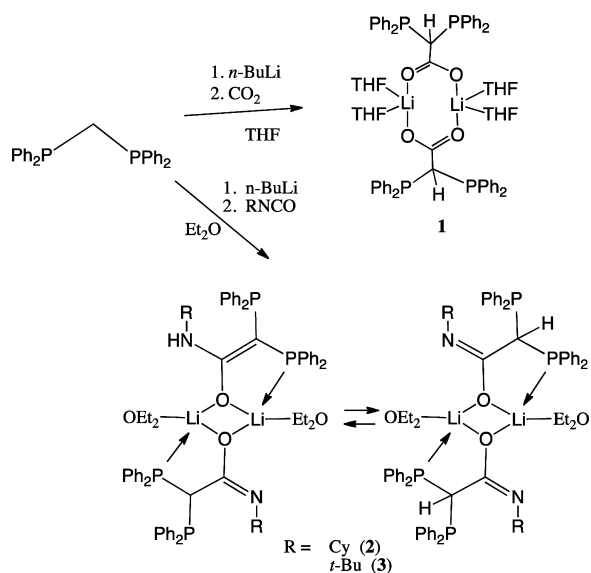
Synthesis of $\{(\text{EtCl}_2\text{Al})\{[(\text{Ph}_2\text{P})_2\text{C}(\text{H})\text{C}=\text{N}(2,4,6\text{-Me}_3\text{C}_6\text{H}_2)\text{-O}]\text{AlEt}_2\}(\mu\text{-Cl})\text{Cr}_2(\mu\text{-Cl})_2\cdot(\text{toluene})\}_2$ (12**).** *Method A.* A suspension of **5** (643 mg, 1 mmol) in THF (30 mL) was mixed with $\text{CrCl}_3(\text{THF})_3$ (1 mmol, 374 mg). After completion of the addition, the solution was stirred for 15 min, producing a dark brown solution. The solvent was then evaporated under vacuum, leaving a brown powder. The powder was dissolved in toluene (30 mL) and mixed with $(\text{CH}_3\text{CH}_2)\text{AlCl}$ (631 mg, 5 mmol). After the addition, the solution was centrifuged and the supernatant liquid was layered with hexanes and allowed to crystallize blue crystals of **12** (0.12 g, 0.13 mmol, 13%). Anal. Calcd (found) for $\text{C}_{88}\text{H}_{108}\text{Al}_4\text{Cl}_8\text{Cr}_2\text{N}_2\text{O}_2\text{P}_4$: C, 57.28 (57.32); H, 5.86 (5.78); N, 1.53 (1.49). $\mu_{\text{eff}} = 3.32\ \mu_{\text{B}}$.

Method B. A suspension of **11** (1.0 g, 1.2 mmol) in toluene (30 mL) was treated with $(\text{CH}_3\text{CH}_2)\text{AlCl}$ (650 mg, 5.3 mmol). After the addition, the solution was centrifuged and the supernatant liquid was layered with hexanes and allowed to crystallize blue crystals of **12** (0.25 g, 0.27 mmol, 45%).

RESULTS AND DISCUSSION

The bis(diphenylphosphino)methane anion (DPPM^-) was prepared in situ by treating commercially available DPPM with 1 equiv of *n*-BuLi in THF or Et_2O . Reacting the anion with CO_2 , CyNCO , and *t*-BuNCO afforded the corresponding lithium salts $\{[(\text{Ph}_2\text{P})_2\text{CHCO}_2]\text{Li}(\text{THF})_2\}_2$ (**1**), $\{[(\text{Ph}_2\text{P})_2\text{C}=\text{CNH}(\text{Cy})\text{O}]\text{Li}(\text{OEt})_2\}_2$ (**2**), and $\{[(\text{Ph}_2\text{P})_2\text{C}=\text{CNH}(\text{t-Bu})\text{O}]\text{Li}(\text{OEt})_2\}_2$ (**3**), respectively (Scheme 1). The $^{31}\text{P}\{^1\text{H}\}$ NMR spectra of the ligands **1–3** showed a single resonance at -16.13 , -12.04 , and -13.9 ppm, respectively, in agreement with the presence of two identical P atoms. In these reactions, the carbon atom located between the two phosphorus atoms of the DPPM^- anion acted as a nucleophile, attacking the electrophilic carbon atom of the cumulenes and in the process forming a carbon–carbon bond. Interestingly, this species may exist in a tautomeric form, where the hydrogen atom may have

Scheme 1



been transferred from the C to the N atom (Scheme 1) and the double bond from the C=N to the C=C position. In the cases of **1** and **2** it was possible to obtain single crystals of suitable quality for X-ray diffraction.

The X-ray structure of **1** consists of a dimer (Figure 1) with two ligand moieties bridged by two tetrahedrally coordinated

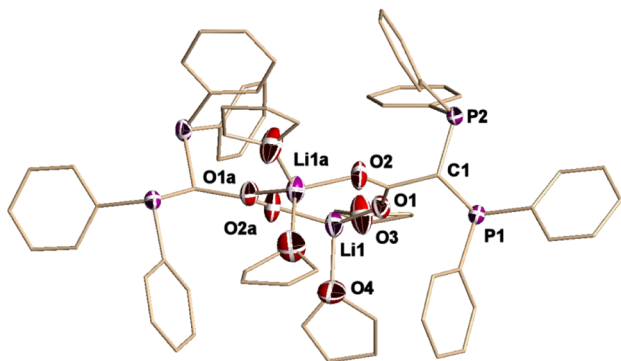


Figure 1. ORTEP drawing of **1**. Selected bond distances (Å) and angles (deg): P(1)–C(1) = 1.866(2), P(2)–C(1) = 1.865(2), C(1)–C(26) = 1.542(3), O(1)–C(26) = 1.245(2), O(2)–C(26) = 1.239(3), Li(1)–O(3) = 1.947(4), Li(1)–O(4) = 1.992(5); O(3)–Li(1)–O(4) = 100.6(2), O(1)–Li(1)–O(2) = 134.6(2), O(1)–Li(1)–O(3) = 103.30(19), O(2)–Li(1)–O(3) = 102.7(2).

lithium atoms. Two of the coordination sites around each lithium are occupied by the oxygen atoms of two THF molecules (Li(1)–O(3) = 1.947(4) Å, Li(1)–O(4) = 1.992(5) Å), while the other two coordination sites are filled by two oxygen atoms, each from one carboxylate moiety (Li(1)–O(1) = 1.891(4) Å, Li(1)–O(2) = 1.991(4) Å).

The structure of **2** (Figure 2) is also dimeric, with two monomeric units linked together by two tetrahedrally coordinated lithium atoms (O(1)–Li(1)–O(2) = 115.4(2)°, O(2)–Li(1)–O(1a) = 113.1(2)°, O(1)–Li(1)–O(1a) = 93.62(18)°, O(2)–Li(1)–P(1a) = 112.80(18)°). Each lithium atom is bonded to two bridging oxygen atom of the isocyanate moieties (Li(1)–O(1) = 1.885(4) Å, Li(1)–O(1a) = 1.904(4) Å), a phosphorus atom (Li(1)–P(1a) = 2.569(4) Å), and one

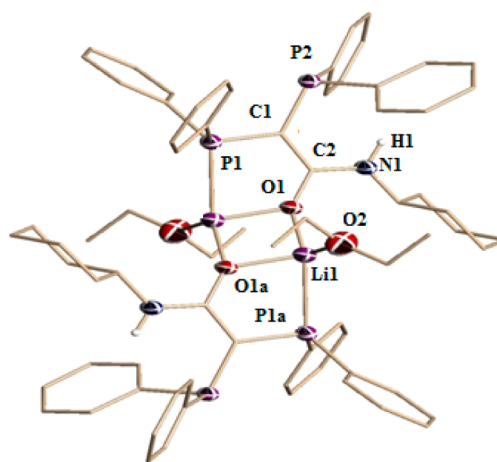


Figure 2. ORTEP drawings of **2**. Selected bond distances (Å) and angles (deg): P(1)–C(1), = 1.784(2), P(2)–C(1) = 1.789(2), C(1)–C(2) = 1.415(3), Li(1)–O(1) = 1.885(4), Li(1)–O(2) = 1.917(5), N(1)–C(2) = 1.359(2), Li(1)–P(1) = 2.569(4); O(2)–Li(1)–O(1a) = 113.1(2), O(1)–Li(1)–O(2) = 115.4(2), O(1)–Li(1)–O(1a) = 93.62(18), O(2)–Li(1)–P(1a) = 112.80(18).

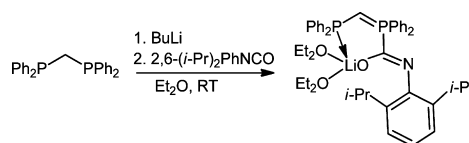
oxygen atom of diethyl ether (Li(1)–O(2) = 1.917(5) Å). The trigonal-planar geometry of the carbon bridging the two phosphorus atoms (P(1)–C(1)–P(2) = 119.14(12)°, C(2)–C(1)–P(1) = 115.11(15)°, C(2)–C(1)–P(2) = 125.48(15)°) and the rather short C–C distance (C(1)–C(2) = 1.415(3) Å) also implies some multiple-bond character with the isocyanate residue carbon atom.

The crystallographic parameters clearly indicate that the hydrogen atom, originally present at the methyne carbon atom of the DPPM[−] anion, has been transferred to the nitrogen atom of the isocyanate, forming an N–H and a C=C bond. The presence of this as a predominant tautomeric form is further confirmed by the absence of methyne correlation peaks in the ¹H{¹³C}-HMQC experiments (see the Supporting Information) and the presence in the ¹H NMR spectrum of a broad peak at 4.8 ppm without carbon correlation characteristic of the N–H function.

When *tert*-butyl isocyanate was used, the lithiated ligand {[Ph₂P)₂C=CNH(*t*-Bu)O]Li(OEt)₂]₂ (**3**), possessing a structure similar to that of **2**, was isolated and fully characterized by NMR. However, when 2,6-diisopropylphenyl isocyanate was employed, the reaction took a different pathway. The structure of the lithium salt [Ph₂PCH=P(Ph₂)C=N(2,6-*i*-Pr₂C₆H₃)O]Li(OEt)₂ (**4**) showed that a nonclassical type of nucleophilic attack of the DPPM[−] phosphorus instead of the carbon atom had occurred (Scheme 2).

This resulted in the formation of a phosphorus–carbon bond instead of the expected carbon–carbon bond. In addition, the formal oxidation state of one of the two phosphorus atoms changed from +3 to +5 as a result of the consequent formation of the C=P double bond within the DPPM[−] anion residue. Accordingly, the ³¹P NMR spectra of the ligand display two

Scheme 2



equally intense peaks at -8.0 and -24.0 ppm, as expected for the presence of two nonequivalent P atoms in different oxidation states.

The crystal structure of **4** (Figure 3) shows the distorted-tetrahedral lithium atom surrounded ($O(2)-Li(1)-O(3) =$

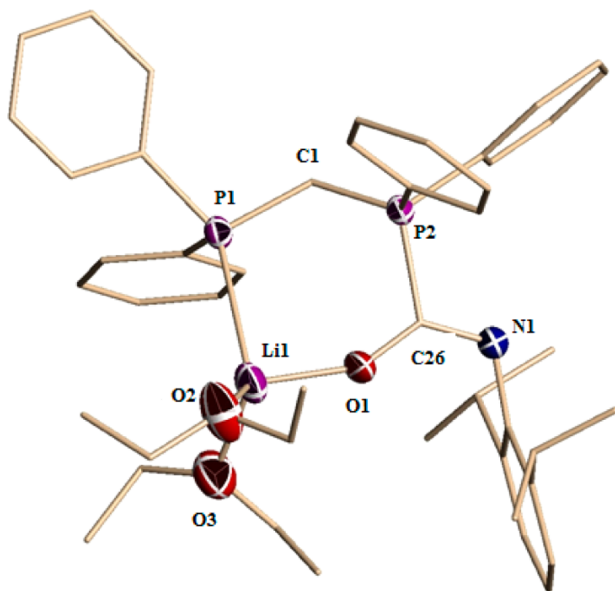


Figure 3. ORTEP drawing of **4**. Ellipsoids are drawn at the 50% probability level, and H atoms are omitted for clarity. Selected bond distances (Å) and angles (deg): $P(1)-C(1) = 1.7510(18)$, $P(2)-C(1) = 1.6932(18)$, $P(2)-C(26) = 1.8557(17)$, $C(26)-O(1) = 1.261(2)$, $N(1)-C(26) = 1.285(2)$; $O(2)-Li(1)-O(3) = 106.75(19)$, $O(1)-Li(1)-O(3) = 109.20(2)$, $O(1)-Li(1)-O(2) = 113.20(2)$, $O(1)-Li(1)-P(1) = 91.03(14)$.

$106.75(19)^\circ$, $O(1)-Li(1)-O(3) = 109.20(2)^\circ$, $O(1)-Li(1)-O(2) = 113.20(2)^\circ$ by one of the two phosphorus atoms ($Li(1)-P(1) = 2.703(4)$ Å), the oxygen atom ($Li(1)-O(1) = 1.813(4)$ Å) of the isocyanate moiety, and two coordinated diethyl ether molecules ($Li(1)-O(2) = 1.948(4)$ Å, $Li(1)-O(3) = 1.977(4)$ Å). The two fairly short²⁰ carbon–phosphorus distances are in agreement with the presence of a significant extent of double-bond character and substantial electronic delocalization within the P–C–P frame ($C(1)-P(1) = 1.751(18)$ Å, $C(1)-P(2) = 1.6932(18)$ Å).

To rationalize the discrepancy of behavior between the aliphatic and aromatic isocyanates, DFT calculations were performed to understand the origin of the nonclassical bonding mode. It was found that the two different bonding modes may be attributed to the different electronic configurations of the two isocyanates (Figure 4) and steric interactions within the final products. The straight $O=C=N-$ functionality of the aromatic isocyanate tends to reside in plane with the rigid aromatic ring, forming a conjugated system. On the other hand, in the case of aliphatic isocyanate, the alkyl group is bent away, allowing the carbon atom to approach the central carbon of the DPPM[−] anion. Instead, the carbon atom of the aromatic isocyanate can only reach the DPPM[−] anion through the phosphorus atom to minimize the steric repulsions.

The behavior of the mesityl derivative $\{[(PPh_2)_2C=CNH(Mes)O]Li\}_n$ (**5**) is in striking contrast with the above arguments. Although single crystals suitable for X-ray analysis could not be grown in this case, the NMR spectra are completely consistent with the classical type of reaction. To

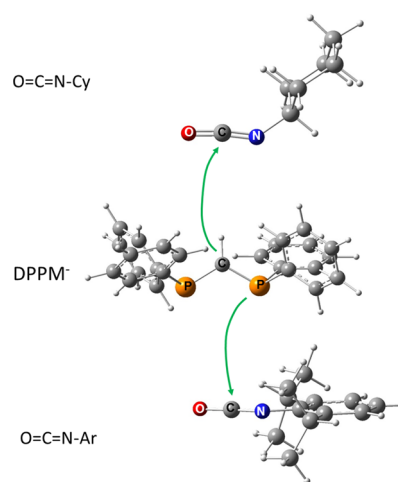


Figure 4. Different approaches of aliphatic and aromatic isocyanates to the DPPM[−] anion (B3LYP-optimized structures).

understand this apparent discrepancy, one must keep in mind the dynamic behavior observed for the two aromatic derivatives (see below). In other words, the mesityl derivative clearly switches the connectivity from classical to nonclassical and back, as a function of the presence of lithium or chromium metal and the aluminate residues (see below). Therefore, it seems reasonable to propose that **5** might possess in the gas phase or the solid state the same structure as the diisopropylphenyl derivative **4**. However, the connectivity might well switch in solution as a result of the solvation and different state of aggregation and solvation of the alkali-metal cation.

To understand the behavior of this family of ligands, we have conducted a preliminary exploration of the behavior of the basic DPPM[−] anion with $CrCl_3(THF)_3$ with variable stoichiometric ratios. The reaction with a 1:1 molar ratio resulted in the formation of the chromium complex $[HC(PPh_2)_2]Cr[(\mu-Cl)_2Li(THF)_2]_2$ (**6**), in which the octahedral coordination sphere of chromium contains one bidentate monoanionic chelating DPPM[−] frame and four chlorine atoms bridging THF-solvated lithium atoms (Figure 5a). However, the reaction of the DPPM[−] anion with 0.5 equiv of $CrCl_3(THF)_3$ afforded the octahedral chromium complex $[HC(PPh_2)_2]_2Cr(\mu-Cl)_2Li(THF)_2 \cdot 1.5THF$ (**7**), whose six coordination sites are occupied by two bidentate-monoanionic chelating DPPM frames and two chlorine atoms bridging THF-solvated lithium atoms (Figure 5b).

The X-ray structures of the two complexes showed similarly distorted octahedral geometries around chromium, with four chlorine atoms bridging between two solvated lithium centers in the case of complex **6** ($Cr(1)-Cl(1) = 2.3500(6)$ Å, $Cr(1)-Cl(2) = 2.3959(6)$ Å). In the case of **7**, only two chlorine atoms bridge between a THF-solvated lithium atom ($Cr(1)-Cl(1) = 2.3634(12)$ Å, $Cr(1)-Cl(2) = 2.3741(12)$ Å). The $Cr(1)-Li(1)$ distance in **6** ($Cr(1)-Li(1) = 3.206(4)$ Å) was found to be slightly shorter than the corresponding bond distance in **7** ($Cr(1)-Li(1) = 3.2989(1)$ Å). In addition, the chromium to phosphorus distances in the case of **6** ($Cr(1)-P(1) = 2.4506(6)$ Å, $Cr(1)-P(1a) = 2.4506(6)$ Å) were shorter than the corresponding bond distances in **7** ($Cr(1)-P(1) = 2.4626(12)$ Å, $Cr(1)-P(3) = 2.4700(12)$ Å, $Cr(1)-P(2) = 2.4978(12)$ Å, $Cr(1)-P(4) = 2.5149(12)$ Å).

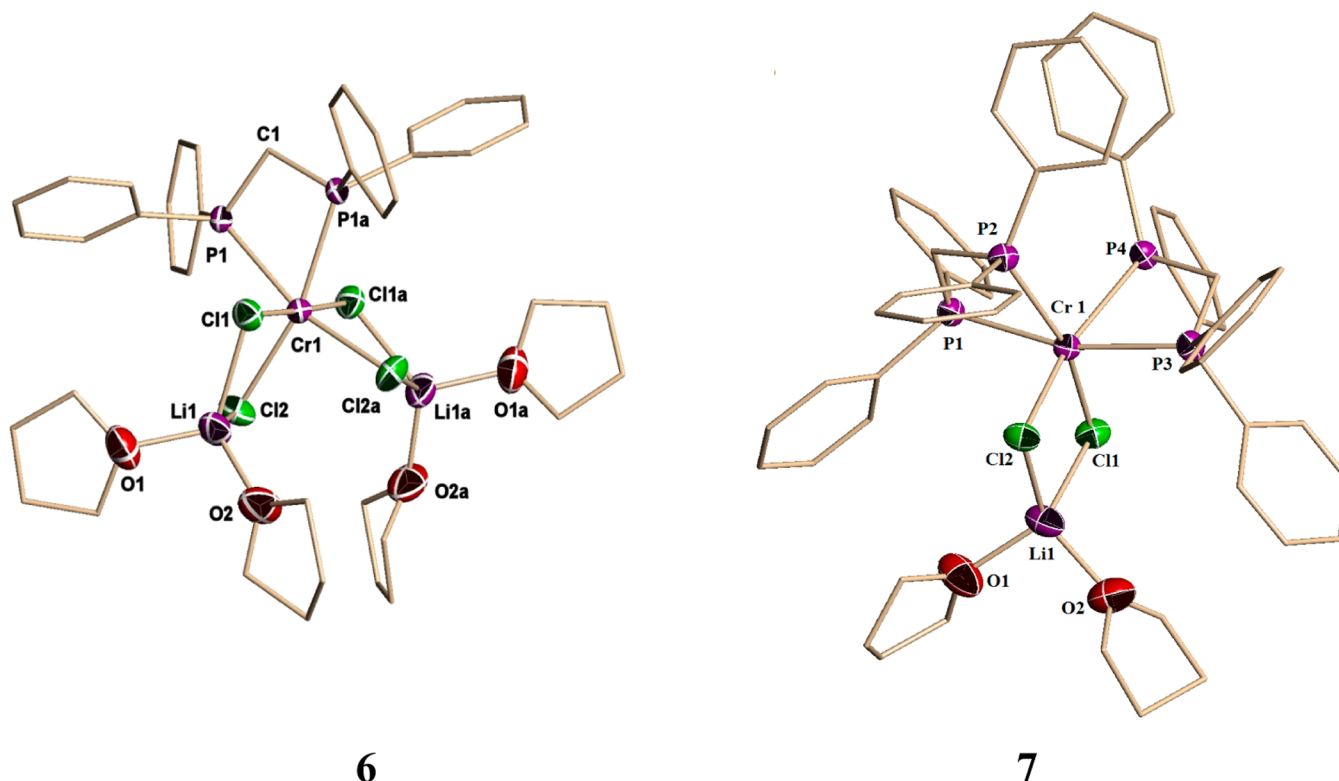


Figure 5. ORTEP drawings of **6** and **7**. Ellipsoids are drawn at the 50% probability level, and H atoms are omitted for clarity. Selected bond distances (Å) and angles (deg) are as follows. For **6**: Cr(1)–Cl(1) = 2.3500(6), Cr(1)–Cl(2) = 2.3959(6), Cr(1)–P(1) = 2.4560(6), Cr(1)–P(1a) = 2.4560(6), P(1)–C(1) = 1.7236; Cl(1)–Cr(1)–Cl(1a) = 177.97(4), Cl(1)–Cr(1)–Cl(2a) = 90.76(2), Cl(1)–Cr(1)–Cl(2) = 90.58(2), Cl(1)–Cr(1)–P(1) = 89.14(2), Cl(1)–Cr(1)–P(1a) = 89.14(2), P(1a)–Cr(1)–P(1) = 67.13(3). For **7**: Cr(1)–Cl(1) = 2.3634(12), Cr(1)–Cl(2) = 2.3741(12), Cr(1)–P(1) = 2.4626(12), Cr(1)–P(2) = 2.4978(12), Cr(1)–P(3) = 2.4700(12), Cr(1)–P(4) = 2.5149(12); Cl(1)–Cr(1)–Cl(2) = 90.31(4), Cl(1)–Cr(1)–P(1) = 95.64(4), Cl(1)–Cr(1)–P(3) = 93.10(4), Cl(1)–Cr(1)–P(4) = 92.52(4).

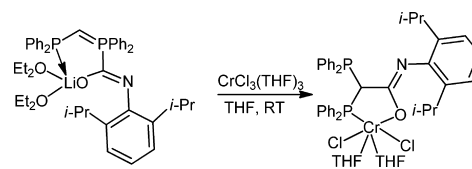
The complexation of $\text{CrCl}_2(\text{THF})_2$ with **1** resulted in the formation of the dimeric chromium complex $[\{[(\text{Ph}_2\text{P})_2\text{C}(\text{H})\text{CO}_2]_2\}\text{Cr}(\text{THF})_2]_2$ (**8**). The molecular structure of **8** (Figure 6) showed a dinuclear chromium complex with a rather short Cr–Cr bond distance (Cr–Cr = 2.337(8) Å) in the characteristic arrangement of the axially coordinated, paddlewheel complexes of divalent chromium.²¹ Four of the coordination sites around each chromium atom are occupied by four oxygen atoms of the carboxylate moiety (Cr(1)–O(3) = 1.9985(18) Å, Cr(1)–O(1) = 2.016(2) Å), while the fifth coordination site is occupied by oxygen atom of the THF molecule (Cr(1)–O(5) = 2.247(2) Å). Complex **8** shows the reduced paramagnetism typical of the paddlewheel divalent chromium dimers ($\mu_{\text{eff}} = 3.91 \mu_{\text{B}}$ per dimer).²¹

Attempts to crystallize complexes of $\text{CrCl}_3(\text{THF})_3$ with **2** invariably led to powdery products. Conversely, reaction of **3** with $\text{CrCl}_3(\text{THF})_3$ afforded $[(\text{Ph}_2\text{P})_2\text{C}(\text{H})\text{C}=\text{N}(t\text{-Bu})\text{O}]\text{CrCl}_2(\text{THF})_2 \cdot 0.5\text{THF} \cdot 0.5(\text{toluene})$ (**9**) in crystalline form. The molecular structure of **9** (Figure 7) showed the octahedral coordination geometry of the chromium atom as defined by one phosphorus (Cr(1)–P(1) = 2.4280(12) Å), one oxygen (Cr(1)–O(1) = 1.937(3) Å), two chlorine atoms (Cr(1)–Cl(1) = 2.2991(12) Å, Cr(1)–Cl(2) = 2.2998(12) Å), and two molecules of THF (Cr(1)–O(2) = 2.069(3) Å, Cr(1)–O(3) = 2.079(3) Å). The long bond distance of the C–C bond connecting the two DPPM[−] and isocyanate residues and the pyramidity of the PCP's C atom indicate that the ligand is present in the tautomeric form containing the C=N double bond and the hydrogen atom on the central carbon of the

DPPM[−] residue. Unfortunately, the isolation of single crystals of the corresponding Cr(II) complex was not successful, due to the poor solubility of this blue microcrystalline material, including in highly polar solvents such as dichloromethane and acetonitrile.

Complexation of ligand **4**, which resulted from a nonclassical isocyanate/diphosphine anion reaction, with $\text{CrCl}_3(\text{THF})_3$ afforded the complex $[(\text{Ph}_2\text{P})\text{C}(\text{H})\text{C}=\text{N}(2,6\text{-}i\text{-Pr}_2\text{C}_6\text{H}_3)\text{O}]\text{CrCl}_2(\text{THF})_2 \cdot 1.5\text{THF}$ (**10**), where the ligand has apparently switched the connectivity toward the classical type of isocyanate–diphosphino anion aggregation (Scheme 3). The

Scheme 3



resulting octahedral chromium complex is very similar to **9**. Accordingly, the phosphorus oxidation state has been reduced from +5 to +3 through an internal redox transformation.

The crystal structure of **10** (Figure 8) shows an octahedrally coordinated chromium atom bonded to one oxygen atom (Cr(1)–O(1) = 1.939(2) Å, O(1)–Cr(1)–Cl(1) = 90.41(7)°) and one phosphorus atom (Cr(1)–P(1) = 2.4334(9) Å, Cl(1)–Cr(1)–P(1) = 91.44(3)°) of the ligand, two chlorine atoms (Cr(1)–Cl(2) = 2.2980(10) Å, Cr(1)–Cl(1) =

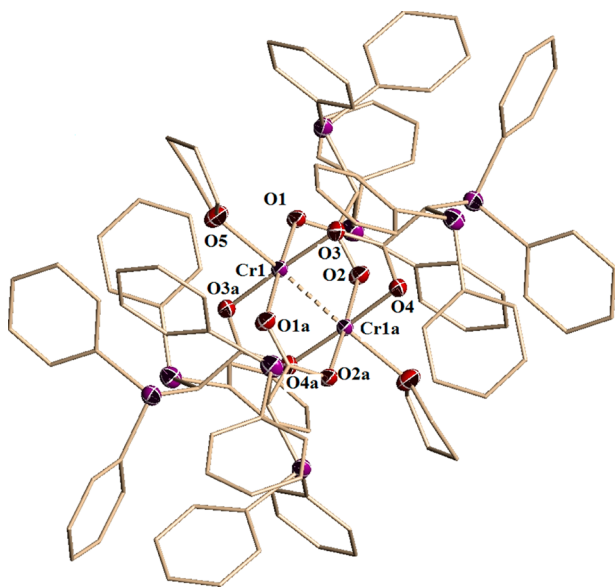


Figure 6. ORTEP drawing of **8**. Ellipsoids are drawn at the 50% probability level, and H atoms are omitted for clarity. Selected bond distances (Å) and angles (deg): Cr(1)–Cr(1a) = 2.3337(8), Cr(1)–O(3) = 1.9985(18), Cr(1)–O(1) = 2.016(2), Cr(1)–O(5) = 2.247(2); O(3)–Cr(1)–O(5) = 89.40(8), O(1)–Cr(1)–O(5) = 91.78(8), O(3)–Cr(1)–O(1) = 93.59(8), O(3)–Cr(1)–O(2) = 86.99(8).

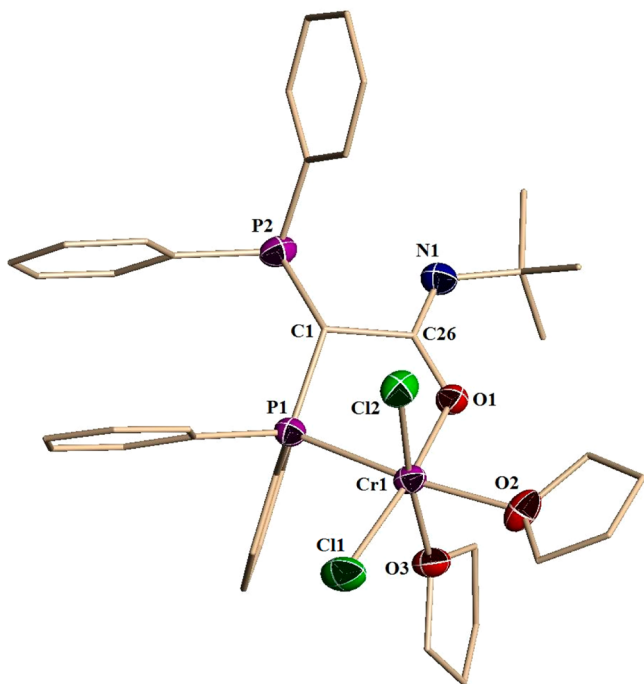


Figure 7. ORTEP drawing of **9**. Ellipsoids are drawn at the 50% probability level, and H atoms are omitted for clarity. Selected bond distances (Å) and angles (deg): Cr(1)–Cl(1) = 2.2991(12), Cr(1)–Cl(2) = 2.2998(12), Cr(1)–P(1) = 2.4280(12), Cr(1)–O(1) = 1.937(3), Cr(1)–O(2) = 2.069(3), Cr(1)–O(3) = 2.079(3), C(1)–C(26) = 1.542(5); O(1)–Cr(1)–Cl(2) = 91.47(8), O(3)–Cr(1)–Cl(2) = 89.71(9), O(1)–Cr(1)–Cl(2) = 91.47(8), Cl(2)–Cr(1)–P(1) = 92.87(4), Cl(2)–Cr(1)–Cl(1) = 91.67(5), O(2)–Cr(1)–Cl(2) = 174.17(9).

2.3016(10) Å, Cl(2)–Cr(1)–Cl(1) = 92.09(4)°, and two THF molecules (O(2)–Cr(1)–Cl(1) = 174.60(8)°). The

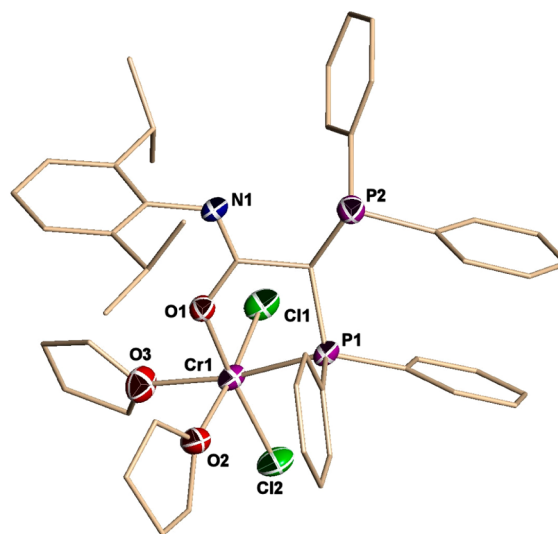


Figure 8. ORTEP drawing of **10**. Ellipsoids are drawn at the 50% probability level, and H atoms are omitted for clarity. Selected bond distances (Å) and angles (deg): P(1)–C(1) = 1.844(3), P(2)–C(1) = 1.870(3), C(1)–C(26) = 1.539(4), Cr(1)–Cl(2) = 2.2980(10), Cr(1)–Cl(1) = 2.3016(10), Cr(1)–O(1) = 1.939(2), Cr(1)–P(1) = 2.4334(9); O(1)–Cr(1)–Cl(1) = 90.41(7), Cl(1)–Cr(1)–P(1) = 91.44(3), O(3)–Cr(1)–Cl(1) = 90.52(9), Cl(2)–Cr(1)–Cl(1) = 92.09(4), O(2)–Cr(1)–Cl(1) = 174.60(8).

change of the phosphorus oxidation state from +5 to +3 is also reflected in the lengthening of P–C bond distances (P(1)–C(1) = 1.844(3) Å, P(2)–C(1) = 1.870(3) Å) in comparison to the corresponding bond distances in the ligand **4** (P(1)–C(1) = 1.751(18) Å, P(2)–C(1) = 1.693(2) Å). Also the C–C bond distance of the link between the isocyanate and diphosphine residues of complex **10** (C(1)–C(26) = 1.539(4) Å) compares well to that of **9** (C(1)–C(26) = 1.542(5) Å). The pyramidity of the PCP's central C atom also indicates the presence of the H atom in that position and consequent C=N double-bond character.

As mentioned above, the behavior of the mesityl analogue is diametrically opposite to that of the diisopropyl derivative. First, the lithium derivative **5** possesses the classical connectivity, as is clearly indicated by the symmetry of its NMR spectra. Second, upon reaction with CrCl₃(THF)₃ and similar to the case of **10**, the ligand connectivity also switched but toward the non-classical form, affording [(Ph₂P)C(H)=P(Ph₂)C=N(2,4,6-Me₃C₆H₂O)]Cr(THF)₂Cl₂ (**11**) (Scheme 4).

Complex **11** is monomeric (Figure 9) with the chromium metal center in a rather regular octahedral coordination (Cl(2)–Cr(1)–O(3) = 89.60(19)°, O(2)–Cr(1)–O(1) = 88.7(3)°, O(1)–Cr(1)–P(1) = 90.77(19)°). Two of the coordination sites are occupied by two chlorine atoms located in a cis orientation with respect to one another (Cl1–Cr1 = 2.274(3) Å, Cl(2)–Cr(1) = 2.313(3) Å, Cl(1)–Cr(1)–Cl(2) = 94.64(11)°). Two oxygen atoms from two molecules of THF occupy two other coordination sites also in cis positions relative to one another (O(2)–Cr(1) = 2.093(7) Å, O(3)–Cr(1) = 2.065(6) Å, O(3)–Cr(1)–O(2) = 85.0(3)°). The final two coordination sites are occupied by an oxygen atom (O(1)–Cr(1) = 1.930(6) Å) and one of the two phosphorus atoms (P(1)–Cr(1) = 2.445(3) Å) of the ligand.

In an attempt to understand the catalytic behavior as a function of the particular nature of the activator (see below),

Scheme 4

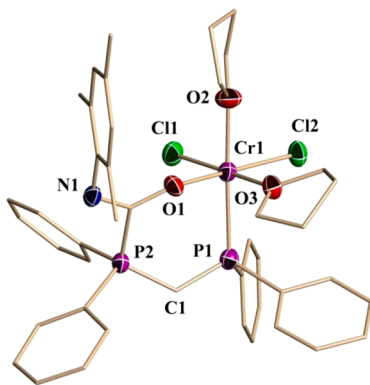
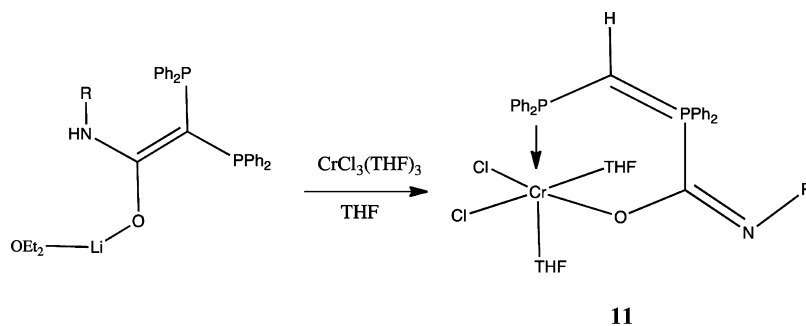


Figure 9. ORTEP drawing of **11**. Ellipsoids are drawn at the 50% probability level, and H atoms are omitted for clarity. Selected bond distances (Å) and angles (deg): O(1)–Cr(1)–P(1) = 90.77(19); P(2)–C(2) = 1.859(9); O(1)–C(2)–N(1) = 128.3(9), O(1)–C(2)–P(2) = 117.9(7), N(1)–C(2)–P(2) = 113.8(7); N(1)–C(2) = 1.283(11), O(1)–C(2) = 1.299(10); P(1)–C(1)–P(2) = 125.0(6); C(1)–P(1) = 1.734(9), C(1)–P(2) = 1.700(10).

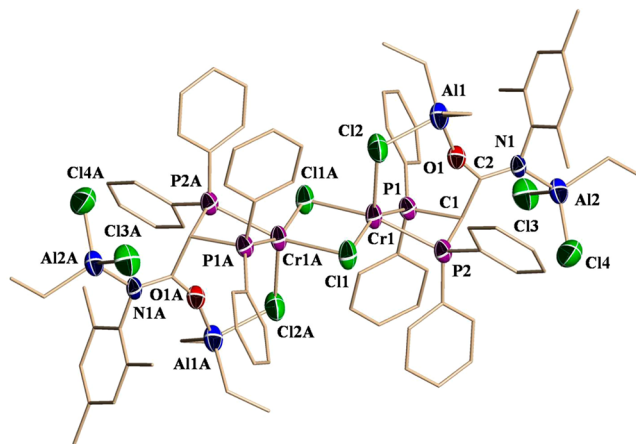


Figure 10. ORTEP drawing of **12**. Ellipsoids are drawn at the 50% probability level, and H atoms are omitted for clarity. Selected bond distances (Å) and angles (deg): Cr(1)–P(2) = 2.480(2); P(2)–C(1)–C(2) = 109.6(4); N(1)–C(2)–C(1) = 122.0(6); Al(1)–O(1) = 1.810(5); Al(2)–N(1) = 1.944(5), Al(2)–Cl(3) = 2.149(3), Al(2)–Cl(4) = 2.142(3), Al(2)–C(6) = 1.922(7).

we have attempted the isolation of complexes as arising from the reaction of **6**–**11** with a variety of aluminum alkyls. The reactions almost invariably afforded very air-sensitive ill-defined materials, often oily in nature. Just in the case of the reaction of **11** with DEAC (Scheme 5), it was possible to isolate a complex in crystalline form formulated as $\{(\text{EtCl}_2\text{Al})[(\text{Ph}_2\text{P})_2\text{C}(\text{H})\text{C}=\text{N}(2,4,6\text{-Me}_3\text{C}_6\text{H}_2)\text{O}(\text{AlEt}_2)](\mu\text{-Cl})\text{Cr}\}_2(\mu\text{-Cl})_2$ (**12**) on the basis of its crystal structure (Figure 10).

The same complex could also be conveniently obtained via one-pot synthesis by reacting **5** with $\text{CrCl}_3(\text{THF})_3$ followed by the addition of DEAC. The salient feature of this species is that the ligand, for the second time, has switched the ligand connectivity from the nonclassical back to the classical. This is a possible result of the retention of the aluminate residue, requiring from the ligand an ampler chelating bite that in turn can be accommodated by a switching of connectivity.

Complex **12** is a symmetry-generated dimer containing two chromium and four aluminum metals. The two square-

pyramidal chromium atoms of each of the two identical units ($\text{Cl}(1)\text{--Cr}(1)\text{--Cl}(1\text{A}) = 92.19(6)^\circ$, $\text{Cl}(1)\text{--Cr}(1)\text{--P}(2) = 95.86(7)^\circ$, $\text{P}(2)\text{--Cr}(1)\text{--P}(1) = 67.93(6)^\circ$, $\text{P}(1)\text{--Cr}(1)\text{--Cl}(2) = 111.78(7)^\circ$) are bridged by two chlorine atoms ($\text{Cr}(1)\text{--Cl}(1) = 2.3763(19)$ Å, $\text{Cr}(1)\text{--Cl}(1\text{A}) = 2.3879(19)$ Å) located on two of the coordination sites of the equatorial plane. A terminally bonded chlorine atom ($\text{Cr}(1)\text{--Cl}(2) = 2.584(2)$ Å) occupying the axial position is in turn bonded to one of the two aluminum atoms ($\text{Cl}(2)\text{--Al}(1) = 2.267(3)$ Å).

Two phosphorus atoms from the DPPM moiety of the ligand chelate the last two equatorial coordination sites of chromium ($\text{Cr}(1)\text{--P}(1) = 2.467(2)$ Å). The central carbon on the DPPM moiety is sp^3 hybridized ($\text{P}(1)\text{--C}(1)\text{--P}(2) = 94.4(3)^\circ$, $\text{P}(1)\text{--C}(1)\text{--C}(2) = 110.5(4)^\circ$), since it is also bonded to one hydrogen atom and to the central carbon atom of the isocyanate moiety ($\text{C}(1)\text{--C}(2) = 1.505(8)$ Å). The carbon on the isocyanate moiety is instead trigonal planar ($\text{O}(1)\text{--}$

Scheme 5

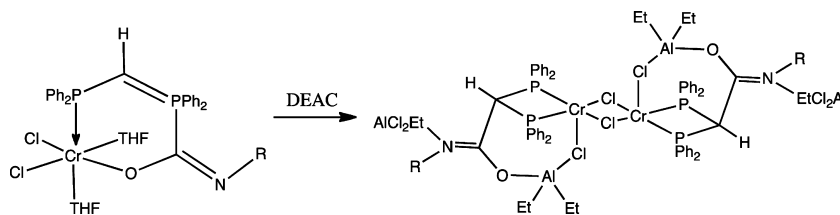


Table 1. Ethylene Oligomerization Results for Complexes 6–12^a

cat. ID (loading, μmol)	cocat. (amt, equiv)	amt of oligomer, mL	amt of PE, g	activity, g/((mmol of Cr) h)	C6, mol %	C8, mol %	$\geq\text{C10}$, mol %	α
6 (30)	MAO (500)	21.7	3.0	1180	48.2	23.6	28.2	0.58
7 (30)	MAO (500)	14.3	0	663	49.8	26.5	23.7	0.55
9 (1)	MAO (300)	21.4	trace	29820	47.4	28.8	23.8	0.60
9 (1)	MAO (500)	17	trace	24000	47.6	29.1	23.1	0.63
9 (1)	MAO (1000)	7.2	4.2	18340	46.8	28.7	24.5	0.69
9 (1)	MAO (1000) + TMA (250)		6.0	12000				
9 (1)	DMAO (500)		1.2	2400				
9 (10) ^b	DMAO (500)		2.2	440				
9 (10) ^b	DMAO (500) + TEA (250)	6.2	2.8	1410	50.7	29.4	19.8	0.65
10 (10)	MMAO (500)		0.7	140				
10 (1)	MAO (500)	6.4	0.5	9520	42.9	31.4	25.2	0.68
10 (1)	MAO (1000)	14.6	0.8	21480	43.7	30.8	25.3	0.65
10 (10)	MMAO (500)		0	0				
10 (10) ^b	DMAO	18.6	0.2	2596	53.5	30	15.63	0.63
11 (10)	DMAO	18.5	0.3	2599	55.0	35.1	9.9	
12 (10)		1.5	0.1	2233	99.9			
12 (10)	DMAO (500) + TEA (250)		traces					

^aOligomerization conditions: solvent, 100 mL of toluene; ethylene pressure, 30 bar; reaction time, 30 min; reaction temperature, 60 °C. ^bThe solvent is methylcyclohexane.

Table 2. Ethylene Oligomerization Results of in Situ Catalyst Testing: 1,2/CrCl₃(THF)₃^a

cat. ID (loading, μmol)	amt of cocat., equiv	amt of oligomer, mL	amt of PE, g	activity, g/((mmol of Cr) h)	C6, mol %	C8, mol %	$\geq\text{C10}$, mol %	α
1 (5)	MAO (500)	12.1	11	7808	47.6	29.1	23.2	0.59
1 (5)	MAO (1000)	18.3	9	8680	48.2	28.7	23.1	0.61
1 (5)	MMAO (500)	7.0	23	11160	44.5	24.9	30.2	0.59
1 (10) ^b	MMAO (500)							
2 (5)	MAO (500)	12.1	0.4	3560	49.1	31.7	18.9	0.62
2 (5)	MAO (1000)	30.4	0.7	8800	53.8	30.2	15.2	0.55
2 (5)	MMAO (500)	6.2		1704	51.9	31.9	16.1	0.53
2 (10) ^b	MMAO							

^aCrCl₃(THF)₃ and 1 or 2 were mixed in toluene and the in situ prepared complexes were injected in the reactor. Reaction conditions: solvent, 100 mL of toluene; ethylene pressure, 30 bar; reaction time, 30 min; reaction temperature, 60 °C. ^bThe solvent is methylcyclohexane.

Table 3. Effect of Catalyst Precursor and Cocatalyst on Selectivity^a

ligand (loading, μmol)	amt of cocat., equiv	amt of oligomer, mL	amt of PE, g	activity, g/((mmol of Cr) h)	C6, mol %	C8, mol %	$\geq\text{C10}$, mol %
1 (1)	DMAO (500)		7.8	15600	0	0	0
1 (1)	DMAO (500)/TEA (100)	9.4	18800	0	0	0	0
2 (5)	DMAO (500)	2.3	6.2	3120	52.8	47.2	0
2 (5)	DMAO (500)/TEA (100)	2.6	9.4	4400	51.9	48.1	0
3 (5)	DMAO (500)	4.5	1.2	1760	61.8	38.9	0
3 (5)	DMAO (500)/TEA (100)	4.9	2.8	2400	61.7	38.3	0
4 (5)	DMAO (500)	2.3	1.9	1400	50.5	49.5	0
4 (5)	DMAO (500)/TEA (100)	2.6	2.4	1600	48.8	51.2	0

^aOligomerization conditions: solvent, 100 mL of methylcyclohexane; ethylene pressure, 30 bar; reaction time, 30 min; reaction temperature, 60 °C; Cr(acac)₃/ligand = 1/1.

C(2)–N(1) = 123.4(6)°, O(1)–C(2)–C(1) = 114.6(6)° with delocalization of the double bond over both the carbon–nitrogen (N(1)–C(2) = 1.306(7) Å) and carbon–oxygen bonds (O(1)–C(2) = 1.295(7) Å). The oxygen of the isocyanate moiety is also bound to the aluminum atom of an Et₂Al unit, which is in turn bonded to the chlorine located at the apical position. The nitrogen atom of the isocyanate moiety is also bonded to the aluminum atom of an EtAlCl₂ residue.

All the chromium complexes were tested for ethylene oligomerization activity under different reaction conditions. The DPPM–chromium complexes 6 and 7, upon activation with MAO in toluene, showed moderate catalytic activity, producing a Schultz–Flory (S-F) distribution of oligomers (Table 1). Complex 7, which contains two monoanionic DPPM ligands, displays a lower catalytic activity (663 g/((mmol of Cr) h)) compared to 6 (1180 g/((mmol of Cr) h))

ligating one DPPM fragment. However, whereas **6** produced a considerable amount of waxy low-molecular-weight PE, **7** was found to be a *polymer-free* oligomerization catalyst under identical reaction conditions. The activity of catalysts **6** and **7** was found to be higher than the activity of the in situ generated DPPM–Cr(III) complex reported by Overett et al.,¹⁷ the poor catalytic performance of which was attributed to the deprotonation of the highly acidic bridging methylene proton by metal alkyl species.²² Both catalysts **6** and **7** were found to be inactive upon activating with different activators such as TEA, DMAO, and MMAO either in toluene or in methylcyclohexane.

The modification of the anionic DPPM framework with isocyanates or CO₂ considerably enhanced the catalytic performance of the complexes (Tables 1–3). Activation of **9** with MAO in toluene resulted in a highly active ethylene oligomerization catalyst, again producing a S-F distribution of oligomers with a maximum activity of 29 820 g/((mmol of Cr) h). Interestingly, not even traces of polymer were detected. The activity and the selectivity of this system was comparable to those of the previously reported NPN system [(*t*-Bu)NP(Ph)₂N(*t*-Bu)]Cr(μ₂-Cl)₂Li(THF)₂, which also showed polymer-free oligomerization behavior.²³ Varying the Al:Cr ratio affected the catalytic activity with a maximum activity at a low Al:Cr ratio. Increasing the Al:Cr ratio had a detrimental effect on the catalytic performance and resulted in the formation of a considerable amount of low-molecular-weight PE. The lower oligomerization activity at higher Al:Cr ratio might be due to the poisoning effect of free TMA present in MAO. Indeed, the addition of 250 equiv of TMA along with MAO switches the catalytic behavior to polymerization, producing polyethylene with a broad molecular weight distribution. Use of DMAO as cocatalyst in methylcyclohexane or in toluene resulted in the formation of different types of PE. In methylcyclohexane, UHMWPE with narrow molecular weight distribution (PDI = 3.2, $M_w = 4.1 \times 10^6$ g/mol) was obtained, while the polymer obtained in toluene showed the characteristic broad molecular weight waxy PE. However, the addition of 250 equiv of TEA along with DMAO in methylcyclohexane resulted in the formation of a S-F distribution of oligomers along with waxy low-molecular-weight PE, implying that yet another different active species is generated upon the addition of TEA. Upon activation with MAO (Al:Cr = 1000), **10** also showed high oligomerization activity (21 480 g/((mmol of Cr) h)). The catalyst was inactive upon activation with MMAO in toluene. However, with DMAO as cocatalyst in methylcyclohexane, **10** showed moderate oligomerization activity. Complexes **10** and **11** display very similar catalytic behavior. As anticipated, complex **12** is a self-activating catalyst producing very small amounts of highly pure 1-hexene. Attempts to boost catalytic activity by adding activators only resulted in catalyst decomposition. This could be understood in terms of competition between the Lewis acidic Cr and Al to coordinate Cl. As a result, the activator could replace Cl and alter the frame of the catalytically active species.²⁴

Since the isolation of well-defined Cr(III) complexes of ligand **1** and **2** were not successful, these ligands were tested in situ by mixing with CrCl₃(THF)₃ and the results are summarized in Table 2.

The in situ generated chromium complex of ligand **1** showed, upon activation with MAO (Al/Cr = 1000) in toluene, an activity of 8680 g/((mmol of Cr) h), producing a S-F distribution of oligomers along with a considerable amount of

PE. It should be noted that 1-butene was not formed by the catalytic cycle. The venting of the reactors was always carried out slowly at low temperature to minimize losses. To our surprise, though, not even traces could be detected. On the other hand, this is in agreement with the work of McGuiness and Gibson indicating that a S-F distribution may also be obtained via a ring expansion mechanism.²⁵ The SEC analysis of the PE showed that it is a low-molecular-weight wax with a narrow molecular weight distribution (PDI = 1.7, $M_w = 2050$ g/mol). When the CrCl₃(THF)₃/**1** system was tested using MMAO as a cocatalyst in toluene, the amount of wax considerably increased (PDI = 1.7, $M_w = 2430$ g/mol) along with small amounts of oligomers. However, the catalyst was completely inactive when the reaction was carried out in methylcyclohexane using MMAO as cocatalyst. The in situ testing of ligand **2** with CrCl₃(THF)₃ also produced a S-F distribution of oligomers at high Al:Cr ratio, with an activity of 8800 g/((mmol of Cr) h), but with less PE formation compared to that for CrCl₃(THF)₃/**1**.

The in situ catalytic testing of ligand **1–4** using Cr(acac)₃ as metal precursor and DMAO as cocatalyst in methylcyclohexane showed some interesting differences (Table 3). The ligand **1** at an Al:Cr ratio of 500 produced only low-molecular-weight wax with a slightly broad polydispersity index (PDI = 5.1, $M_w = 12\,000$ g/mol). The IR analysis of the resulting PE showed that it is vinyl terminated. The addition of 100 equiv of TEA along with DMAO only increased the amount of PE. Interestingly, whereas **9** and **10** produced a S-F distribution of oligomers, on activation with DMAO (+TEA) the combination of Cr(acac)₃ and ligands **2–4** produced 1-hexene/1-octene selective catalysts (no higher liquid oligomers), albeit with a considerable amount of low-molecular-weight waxes. The formation of a higher amount of wax in comparison to the amount of hexene and octene might be due to the predominant stabilization of divalent chromium compared to the monovalent oxidation state. Ligand **3** showed slightly higher oligomerization activity. The addition of TEA as an external alkylating agent/reducing agent did not result in any considerable improvement in terms of oligomerization activity and selectivity; it only helped to increase the amount of wax in all cases.

CONCLUSIONS

Attempts to functionalize the DPPM[−] anions by reaction with isocyanates afforded new ligands displaying a nonanticipated dynamism. Aside from the expected nucleophilic attack of the negatively charged C atom at the C of the cumulenes, in some cases it was the P atom that acted as a nucleophile, producing ligands with a different connectivity (nonclassical). However, the connectivity may switch back and forward between the two classical and nonclassical forms depending on the steric requirements of the final complexes. While we found no evidence that this may be a fluxional behavior (at least in the case of the diamagnetic lithium salt), this strange ligand dynamism in principle holds some promises for catalysis. To this end, the catalytic testing on all the chromium species presented in this work showed mainly nonselective behavior. Use of Cr(acac)₃ as metal precursor and DMAO as cocatalyst in methylcyclohexane resulted in the formation of 1-hexene and 1-octene (no higher liquid oligomers) along with low-molecular-weight polyethylene wax. Only in the case of complex **12** was an interesting selective and self-activating behavior obtained. The fact that the complex possesses Cr in its

divalent state implies further reduction during the self-activation process.

■ ASSOCIATED CONTENT

■ Supporting Information

A figure, tables, and CIF files giving the ^1H - ^{13}C HMQC spectrum of ligand **2**, crystallographic data for all crystal structures given in the paper, and Cartesian coordinates for the calculated structures. This material is available free of charge via the Internet at <http://pubs.acs.org>.

■ AUTHOR INFORMATION

Corresponding Author

*E-mail: sgambaro@uottawa.ca (S.G.).

Notes

The authors declare no competing financial interest.

■ ACKNOWLEDGMENTS

This work was supported by the Natural Science and Engineering Council of Canada (NSERC) and the Dutch Polymer Institute (DPI, #638), Eindhoven, The Netherlands.

■ REFERENCES

- (1) Vogt, D. *Applied Homogeneous Catalysis with Organometallic Compounds*; Cornils, B., Herrmann, W. A., Eds.; Wiley-VCH: Weinheim, Germany, 1996; Vol. 1, p 245.
- (2) (a) Reagan, W. K. (Phillips Petroleum Company) EP 0417477, 1991. (b) Knudsen, R. D.; Freeman, J. W.; Lashier, M. E. (Phillips Petroleum Company) US 5563312, 1996. (c) Freeman, J. W.; Buster, J. L.; Knudsen, R. D. (Phillips Petroleum Company) US 5856257, 1999. (d) Reagan, W. K.; Freeman, J. W.; Conroy, B. K.; Pettijohn, T. M.; Benham, E. A. (Phillips Petroleum Company) EP 0608447, 1994.
- (3) (a) McGuinness, D. S.; Wasserscheid, P.; Keim, W.; Morgan, D. H.; Dixon, J. T.; Bollmann, A.; Maumela, H.; Hess, F. M.; Englert, U. *J. Am. Chem. Soc.* **2003**, *125*, 5272. (b) Dixon, J. T.; Wasserscheid, P.; McGuinness, D. S.; Hess, F. M.; Maumela, H.; Morgan, D. H.; Bollmann, A. (Sasol Technology (Pty) Ltd) WO 03053890, 2001. (c) McGuinness, D. S.; Wasserscheid, P.; Keim, W.; Hu, C.; Englert, U.; Dixon, J. T.; Grove, C. *Chem. Commun.* **2003**, 334.
- (4) (a) Wass, D. F. (BP Chemicals Ltd) WO 02/04119, 2002. (b) Carter, A.; Cohen, S. A.; Cooley, N. A.; Murphy, A.; Scutt, J.; Wass, D. F. *Chem. Commun.* **2002**, 858.
- (5) (a) Zhang, J.; Braunstein, P.; Hor, A. T. S. *Organometallics* **2008**, *27*, 4277.
- (6) (a) Agapie, T. *Coord. Chem. Rev.* **2011**, *255*, 861. (b) McGuinness, D. S. *Chem. Rev.* **2011**, *111*, 2321 and references therein. (d) Wass, D. F. *Dalton Trans.* **2007**, 816.
- (7) (a) Bollmann, A.; Blann, K.; Dixon, J. T.; Hess, F. M.; Killian, E.; Maumela, H.; McGuinness, D. S.; Morgan, D. H.; Neveling, A.; Otto, S.; Overett, M.; Slawin, A. M. Z.; Wasserscheid, P.; Kuhlmann, S. *J. Am. Chem. Soc.* **2004**, *126*, 14712. (b) Han, T. K.; Ok, M. A.; Chae, S. S.; Kang, S. O. (SK Energy Corporation), WO 2008/ 088178, 2008. (c) Shaikh, E.; Albahily, K.; Sutcliffe, M.; Fomitcheva, V.; Gambarotta, S.; Duchateau, R.; Korobkov, I. *Angew. Chem., Int. Ed.* **2012**, *51*, 1. (d) Licciulli, S.; Thapa, I.; Albahily, K.; Korobkov, I.; Gambarotta, S.; Duchateau, R.; Chevalier, R.; Schuhen, K. *Angew. Chem., Int. Ed.* **2010**, *49*, 9225.
- (8) (a) Manyik, R. M.; Walker, W. E.; Wilson, T. P. *J. Catal.* **1977**, *47*, 197. (b) Briggs, J. R. *Chem. Commun.* **1989**, *11*, 674. (c) McDermott, J. X.; White, J. F.; Whitesides, G. M. *J. Am. Chem. Soc.* **1973**, *95*, 4451. (d) McDermott, J. X.; White, J. F.; Whitesides, G. M. *J. Am. Chem. Soc.* **1976**, *98*, 6521. (e) Agapie, T.; Labinger, J. A.; Bercaw, J. E. *J. Am. Chem. Soc.* **2007**, *129*, 14281. (f) Agapie, T.; Schofer, S. J.; Labinger, J. A.; Bercaw, J. E. *J. Am. Chem. Soc.* **2004**, *126*, 1304. (g) Tomov, A. K.; Chirinos, J. J.; Long, R. J.; Gibson, V. C.; Elsegood, M. R. *J. Am. Chem. Soc.* **2006**, *128*, 7704. (h) McGuinness,

- D. S.; Suttill, J. A.; Gardiner, M. G.; Davies, N. W. *Organometallics* **2008**, *27*, 4238. (i) Rensburg, W. J.; Grove, C.; Steynberg, J. P.; Stark, K. B.; Huysen, J. J.; Steynberg, P. J. *Organometallics* **2004**, *23*, 1207. (j) Blom, B.; Klatt, G.; Fletcher, J. C. Q.; Moss, J. R. *Inorg. Chim. Acta* **2007**, *360*, 2890. (k) Bhaduri, S.; Mukhopadhyay, S.; Kulkarni, S. A. *J. Organomet. Chem.* **2009**, *694*, 1297.
- (9) (a) Temple, C.; Jabri, A.; Crewdson, P.; Gambarotta, S.; Korobkov, I.; Duchateau, R. *Angew. Chem.* **2006**, *118*, 7208. (b) Jabri, A.; Temple, C.; Crewdson, P.; Gambarotta, S.; Korobkov, I.; Duchateau, R. *J. Am. Chem. Soc.* **2006**, *128*, 9238. (c) Jabri, A.; Crewdson, P.; Gambarotta, S.; Korobkov, I.; Duchateau, R. *Organometallics* **2006**, *25*, 715. (d) Zhang, J.; Li, A.; Hor, T. S. A. *Organometallics* **2009**, *28*, 2935.
- (10) (a) Kohn, R. D.; Haufe, M.; Mihan, S.; Lilge, D. *Chem. Commun.* **2000**, 1927. (b) Fang, Y.; Liu, Y.; Ke, Y.; Guo, C.; Zhu, N.; Mi, X.; Ma, Z.; Hu, Y. *Appl. Catal., A* **2002**, *235*, 33. (c) Yang, Y.; Liu, Z.; Zhong, L.; Qiu, P.; Dong, Q.; Cheng, R.; Vanderbilt, J.; Liu, P. *Organometallics* **2011**, *30*, 5297. (d) Rucklidge, A. J.; McGuinness, D. S.; Tooze, R. P.; Slawin, A. M. Z.; Pelletier, J. D. A.; Hanton, M. J.; Webb, P. B. *Organometallics* **2007**, *26*, 2782.
- (11) (a) Morgan, D. H.; Schwikkard, S. L.; Dixon, J. T.; Nair, J. J.; Hunter, R. *Adv. Synth. Catal.* **2003**, *345*, 939. (b) Van Rensburg, W. J.; Grove, C.; Steynberg, J. P.; Stark, K. B.; Huysen, J. J.; Steynberg, P. J. *Organometallics* **2004**, *23*, 1207.
- (12) Meijboom, N.; Schaverien, C. J.; Orpen, A. G. *Organometallics* **1990**, *9*, 774.
- (13) (a) Vidyaratna, I.; Nikiforov, G. B.; Gorelsky, S. I.; Gambarotta, S.; Duchateau, R.; Korobkov, I. *Angew. Chem., Int. Ed.* **2009**, *48*, 6552. (b) Albahily, K.; Fomitcheva, V.; Murugesu, M.; Gambarotta, S.; Korobkov, I.; Gorelsky, S. I. *J. Am. Chem. Soc.* **2011**, *133*, 6388.
- (14) (a) Peitz, S.; Peulecke, N.; Aluri, B. P.; Hansen, S.; Müller, B. H.; Spannenberg, A.; Rosenthal, U.; Al-Hazmi, M. H.; Mosa, F. M.; Wöhl, A.; Müller, W. *Eur. J. Inorg. Chem.* **2010**, 1167. (b) Wöhl, A.; Müller, W.; Peitz, S.; Peulecke, N.; Aluri, B. P.; Müller, B. H.; Heller, D.; Rosenthal, U.; Al-Hazmi, M. H.; Mosa, F. M. *Chem. Eur. J.* **2010**, *16*, 7833. (c) Peitz, S.; Peulecke, N.; Müller, B. H.; Spannenberg, A.; Drexler, H. J.; Rosenthal, U.; Al-Hazmi, M. H.; Al-Eidan, K. E.; Wöhl, A.; Müller, W. *Organometallics* **2011**, *30*, 2364. (d) Aluri, B. R.; Peulecke, N.; Peitz, S.; Spannenberg, A.; Müller, B. H.; Schulz, S.; Drexler, H. J.; Heller, D.; Al-Hazmi, M. H.; Mosa, F. M.; Wöhl, A.; Müller, W. *Dalton Trans.* **2010**, *39*, 7911. (e) Peitz, S.; Peulecke, N.; Aluri, B. R.; Müller, B. H.; Spannenberg, A.; Rosenthal, U.; Al-Hazmi, M. H.; Mosa, F. M.; Wöhl, A.; Müller, W. *Organometallics* **2010**, *29*, 5263.
- (15) (a) Albahily, K.; Koc, E.; Al-Baldawi, D.; Savard, D.; Gambarotta, S.; Burchell, T. J.; Duchateau, R. *Angew. Chem., Int. Ed.* **2008**, *47*, 5816. (b) Albahily, K.; Koc, E.; Al-Baldawi, D.; Savard, D.; Gambarotta, S.; Burchell, T. J.; Duchateau, R. *Angew. Chem., Int. Ed.* **2008**, *47*, 5816. (c) Albahily, K.; Al-Baldawi, D.; Gambarotta, S.; Koc, E.; Duchateau, R. *Organometallics* **2008**, *27*, 5708. (d) Albahily, K.; Al-Baldawi, D.; Gambarotta, S.; Koc, E.; Duchateau, R. *Organometallics* **2008**, *27*, 5943.
- (16) (a) Thapa, I.; Gambarotta, S.; Duchateau, R.; Kulangara, S. V.; Chevalier, R. *Organometallics* **2010**, *29*, 4080.
- (17) (a) Overett, M. J.; Blann, K.; Bollmann, A.; Villiers, R.; Dixon, J. T.; Killian, E.; Maumela, M. C.; Maumela, H.; McGuinness, D. S.; Morgan, D. H.; Rucklidge, A.; Slawin, M. Z. A. *J. Mol. Catal. A: Chem.* **2008**, *283*, 114.
- (18) Dulai, A.; de Bod, H.; Hanton, M. J.; Smith, D. M.; Downing, S.; Mansell, S. M.; Wass, D. F. *Organometallics* **2009**, *28*, 4613.
- (19) Kern, R. J. *J. Inorg. Nucl. Chem.* **1962**, *24*, 1105.
- (20) (a) Zhang, S.; Pattacini, R.; Braunstein, P. *Inorg. Chem.* **2011**, *50*, 3511. (b) Block, M.; Kluge, T.; Bette, M.; Schmidt, J.; Steinborn, D. *Organometallics* **2010**, *29*, 6749.
- (21) Edema, J.; Gambarotta, S. *Comments Inorg. Chem.* **1991**, *11*, 195.
- (22) Al-Jibori, S.; Shaw, B. L. *J. Chem. Soc., Chem. Commun.* **1982**, 286.

(23) Albahily, K.; Licciulli, S.; Gambarotta, S.; Korobkov, I.; Chevalier, R.; Schuhen, K.; Duchateau, R. *Organometallics* **2011**, *30*, 3346.

(24) Müller, B. H.; Peulecke, N.; Peitz, S.; Aluri, B. P.; Rosenthal, U.; Al-Hazmi, M. H.; Mosa, F. M.; Wöhl, A.; Müller, W. *Chem. Eur. J.* **2011**, *17*, 6935.

(25) (a) Tomov, A. K.; Chirinos, J. J.; Long, R. J.; Gibson, V. C.; Elsegood, M. R. *J. Am. Chem. Soc.* **2006**, *128*, 7704. (b) Tomov, A. K.; Chirinos, J. J.; Jones, D. J.; Long, R. J.; Gibson, V. C. *J. Am. Chem. Soc.* **2005**, *127*, 10166.